

## A Top-down Approach to S-UTD-CH Model

**Mehmet B. Tabakcioglu**

Electrical and Electronics Engineering Department  
Bursa Technical University, Bursa, 16330, Turkey  
mehmet.tabakcioglu@btu.edu.tr

**Abstract** — Free space electromagnetic wave propagation is an excessively pretty simple. However, in the reality, there are obstructions like buildings and hills blocking the electromagnetic waves and leading diffraction and reflection, and these obstructions can be modeled as a knife edge or wedge due to using of UHF. Hence, the vital problem is how an electromagnetic wave propagates in multiple diffraction scenario including buildings, trees, hills, cars etc. In order to estimate the field strength or relative path loss of the waves at the receiver, so many electromagnetic wave propagation models have been introduced throughout the century. Ray tracing and numerical integration based propagation models are introduced. In this paper, detailed information is provided about S-UTD-CH (Slope UTD with Convex Hull) model. Particularly, in the transition zone, the S-UTD-CH model can be applied to multiple diffraction scenarios. In addition, Fresnel zone concept, convex hull and slope UTD models are fundamentals of the S-UTD-CH model. Moreover, in terms of computation time and accuracy, the S-UTD-CH model is conceived an optimum model. Furthermore, verification of S-UTD-CH model is made by means of FEKO, which is a comprehensive electromagnetic simulation software tool by Altair.

**Index Terms** — Diffraction, FEKO, radio wave propagation, Ray-tracing, S-UTD-CH model.

### I. INTRODUCTION

In order to establish high precision and time efficient communication networks and radio broadcasting systems too many electromagnetic wave propagation models have been introduced throughout the century. At first, geometrical optic model observing some physical events like reflection, refraction and enlightenment is proposed [1]. The geometrical optic (GO) model based on particle property of the light. That is, the light propagates from the source as particle and there are sharp shadow boundaries. The geometrical optic model does not work successfully in the case of multiple-diffraction. In real environment, there are obstacles such as buildings, hills, trees and cars etc., can cause reflection, refraction and diffraction. Thanks to using ultra-high frequency (UHF)

electromagnetic waves, the buildings, trees and hills in the environment can be modeled as knife edge and wedge structures, respectively. Geometrical theory of diffraction (GTD) model is introduced by Keller [2]. The GTD model is an extension to the GO model by adding diffracted waves [3]. The GTD model fails to calculate the field strength in the vicinity of the optical boundaries [4]. In other words, the GTD model is unsuccessful to calculate the relative path loss in the case of that source, diffraction and observation points are in the same line [5]. The GTD model finds the acceptable results in the case that the size of obstacle is less than the wavelength of the incident wave [6]. In 1966, Deygout proposed a new multiple-diffraction propagation model for knife-edge structures [7]. This model is valid for the environment including limited number of knife-edge structures [8]. Besides this model fails to calculate the relative path loss in the case of that the knife edges are close to each other [9]. Uniform theory of diffraction (UTD) model is a high frequency asymptotic technique introduced by [10] and computes the field strength at the receiver in a very short time. The UTD model removes some of the failure of GTD model in the vicinity of the shadow boundary. If an obstacle blocks the frontal path loss accurately [11, 12]. That is, if the heights of the obstacles are close to each other, the UTD model gives inaccurate predictions. In order to remove the failure of the UTD model, slope UTD model is proposed [13-16]. This model is more exact than the GO, GTD and UTD models. It is based on adding of derivatives of incident fields. Some simulations are made in order to verify the S-UTD model with Vogler's model [17]. Vogler model is an accurate and numerical integration based well-known model. If the number of obstacle is greater than 10, the S-UTD model fails to predict the field strength accurately, and leads so much complexity and requires so much computation time. That is, up to 10 diffractions, the S-UTD model come up with remarkable, accurate, meaningful and time-efficient results [18-20]. In order to overcome time efficiency and exactness deficiencies of slope UTD model, another UTD-based, ray theoretical, time-efficient and accurate model is proposed [19-23].

The proposed model called by S-UTD-CH, abbreviated form of Slope UTD with Convex Hull. In fact S-UTD-CH model is not a new model and only combination of the Slope UTD model and Convex-Hull model. The rest of paper explains S-UTD-CH model and give comparison results of UTD based models with regard to computation time and accuracy of prediction. Another comparison is made by using CAD FEKO electromagnetic simulation software tool.

## II. S-UTD-CH MODEL

Electric field behind an obstacle can be calculated by formula in [24]:

$$E = \left[ E_i D + \frac{\partial E_i}{\partial n} d_s \right] A(s) e^{-jks}, \quad (1)$$

where  $E_i$  is incident field,  $A(s)$  is the spreading factor,  $D$  is the amplitude diffraction coefficient,  $k$  is the wave number,  $d_s$  is the slope diffraction coefficient,  $n$  represents the normal and  $s$  is a distance. The obstacles like buildings and hills can be modelled as a knife edge, wedge or cylinder thanks to using UHF waves. In the knife-edge case diffraction coefficient [16] is expressed by:

$$D(\alpha) = - \frac{e^{-j\pi/4}}{2\sqrt{2\pi k \cos(\alpha/2)}} F[x], \quad (2)$$

where,  $k$  is the wave number,  $F[x]$  is the transition function given in [25],  $\alpha$  is an angle between the incident and the diffracted waves.  $A(s)$  is the spreading factor is given by:

$$A(s) = \sqrt{\frac{s_0}{s_1(s_1+s_0)}}, \quad (3)$$

where,  $s_0$  is the total distance before the last diffracting obstacle, whereas  $s_1$  is the distance after the last diffracting obstacle as shown in Fig. 1.

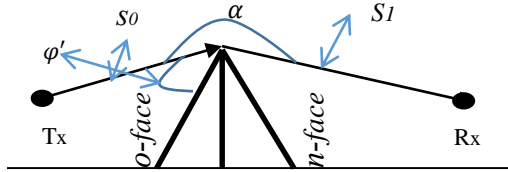


Fig. 1. Diffraction geometry.

By taking into account the wedge structure, polarisation effects have to be added. The amplitude diffraction coefficients [26] for horizontal and vertical polarization are given by:

$$D_s = R_{0s} R_{ns} D_1 + D_2 + R_{0s} D_3 + R_{ns} D_4, \quad (4)$$

$$D_h = R_{0h} R_{nh} D_1 + D_2 + R_{0h} D_3 + R_{nh} D_4, \quad (5)$$

where,  $h$  and  $s$  indices stand for vertical and horizontal polarisations.  $R$  is the reflection coefficient,  $o$  and  $n$  denote zero and  $n$  faces of the wedge and they are illustrated in Fig. 1.

$D_{1,2,3,4}$  are in [27] are given by:

$$D_i = \frac{-e^{-j\pi/4}}{2n\sqrt{2\pi k}} \cot(\psi(i)) F(2kLn^2 \sin^2(\psi(i))), \quad (6)$$

$\psi(1) = \frac{\pi+\varphi-\varphi'}{2n}$ ,  $\psi(2) = \frac{\pi-\varphi+\varphi'}{2n}$ ,  $\psi(3) = \frac{\pi-\varphi-\varphi'}{2n}$ ,  $\psi(4) = \frac{\pi+\varphi+\varphi'}{2n}$ , where,  $n$  is a number ( $n = 2 - \beta/\pi$ ) ranging in  $[0-2]$ .  $\beta$  is the internal angle and  $L$  is the distance parameter calculated via using continuity equations.

Due to using wedge structure, the reflected fields have to be taken into account. Thus, the reflection coefficients in [28] are given by:

$$R_{0s} = \frac{\sin(\varphi') - \sqrt{\varepsilon_r - \cos^2(\varphi')}}{\sin(\varphi') + \sqrt{\varepsilon_r - \cos^2(\varphi')}}, \quad (7)$$

$$R_{0h} = \frac{\varepsilon_r \sin(\varphi') - \sqrt{\varepsilon_r - \cos^2(\varphi')}}{\varepsilon_r \sin(\varphi') + \sqrt{\varepsilon_r - \cos^2(\varphi')}}, \quad (8)$$

$$R_{ns} = \frac{\sin(n\pi - \varphi) - \sqrt{\varepsilon_r - \cos^2(n\pi - \varphi)}}{\sin(n\pi - \varphi) + \sqrt{\varepsilon_r - \cos^2(n\pi - \varphi)}}, \quad (9)$$

$$R_{nh} = \frac{\varepsilon_r \sin(n\pi - \varphi) - \sqrt{\varepsilon_r - \cos^2(n\pi - \varphi)}}{\varepsilon_r \sin(n\pi - \varphi) + \sqrt{\varepsilon_r - \cos^2(n\pi - \varphi)}}, \quad (10)$$

As aforementioned, the S-UTD-CH model is combination of two previously proposed S-UTD (Slope UTD) and CH (Convex Hull) models. Convex hull model is introduced and applied in [29, 30]. A convex hull is constructed by using the Fresnel zone. The Fresnel zone, an ellipsoid region between the transmitting and receiving antennas, is commonly used in radio planning tools [31] as depicted in Fig. 2.

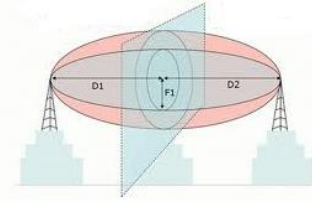


Fig. 2. Fresnel zone.

$F_1$  is the radius of the first Fresnel zone expressed by:

$$F_1 = \sqrt{\frac{ncD_1D_2}{f(D_1+D_2)}}, \quad (11)$$

where ( $n=1$ ) is the order of the Fresnel zone and  $c$  is the speed of light,  $D_1$  and  $D_2$  are the distance before and after the obstacle, respectively.

Most of the wave emits from the transmitter propagates in Fresnel zone. If the obstacle does not disrupt the Fresnel zone, this obstacle would be excluded from the scenario due to so little contribution on the receiver. Fresnel zone disruption by tree and house can be seen in Fig. 3.

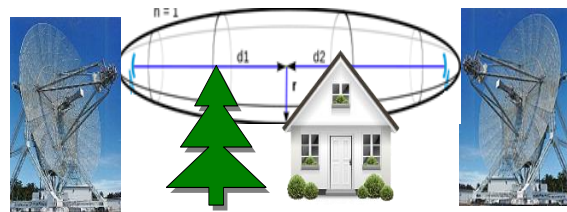


Fig. 3. Fresnel zone disruption.

Convex hull, a polygon between the transmitter and the receiver, is constructed by using the fresnel zone concept [32].

Firstly, the first fresnel zone is drawn between the transmitter and the receiver. Some obstacles placed outside of the zone are excluded from the scenario. Then, the highest obstacle intersecting the line between the transmitter and the receiver in the scenario is selected. Next, secondary fresnel zones are drawn between the transmitter and the highest obstacle and between the receiver and the highest obstacle. After that, the obstacles placed outside of the secondary zones are excluded from the scenario again. Finally, convex hull is constructed with remained obstacles as illustrated in Figs. 4 (a-b).

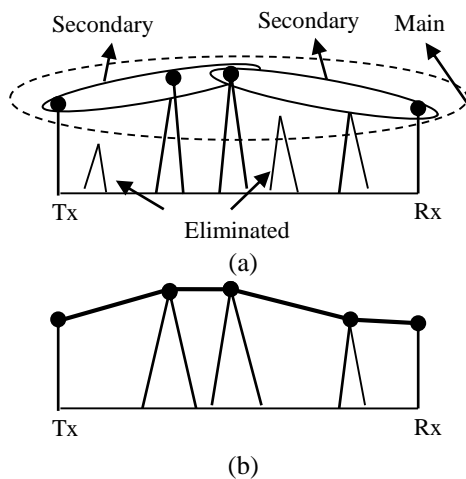


Fig. 4. Convex hull construction.

Exclusion of some unsuccessful diffracting obstacles alleviates the computation time and complexity by not promising from the accuracy of predicted field.

S-UTD-CH mechanism can be explained as followed. Firstly, convex hull is constructed by utilising the Fresnel zone concept. Secondly, all the ray paths emanate from the transmitter and ends on the receiver are determined. Finally, Slope UTD model runs for these ray paths and predicts the field strength.

### III. COMPARISON OF THE MODELS

A lot of comparisons have been carried out among the models for accuracy and/or computation time [33-38]. Ray-theoretical electromagnetic wave propagation models, which are UTD, S-UTD and S-UTD-CH, are compared with regard to computation time and accuracy of prediction of relative path loss in this section. In the case of that there are fewer than 11 diffractions in the scenario the S-UTD model is envisioned the reference model according to accuracy of prediction. The scenario of comparisons is illustrated in Fig. 5.

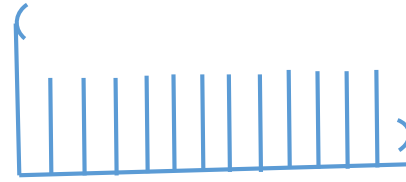


Fig. 5. Test scenarios for comparison.

As shown in Fig. 5, there are 10 obstacles in given scenario, and the obstacles and the receiving antenna heights are 20 m and 1.5 m, respectively. All the distances between obstacles and antennas are deployed equally spaced as 25 m and 50 m. The operational frequencies are 100, 400, 900 and 1800 MHz. The height of transmitter is selected as 10, 15, 20, 25 and 30 m.

In the first case, the operational frequency is 100 MHz and the distance between the obstacles is 25 m. The transmitter heights are selected as 10, 15, 20, 25 and 30 m, respectively. In order to show how the relative path loss is affected by the change of transmitter height, simulation is performed, and the results are demonstrated in Table 1.

In Table 1, the first column shows the transmitter height. Next three columns indicate the relative path loss of S-UTD-CH, S-UTD and UTD models, respectively. The latter three columns give the computation time of mentioned models. The eliminated obstacle number in the S-UTD-CH model is shown in the last column.

The UTD model requires the least computation time. Also, in the highly elevated transmitting antenna case (30 m), due to one obstacle elimination the S-UTD-CH model has relatively shorter computation time than S-UTD model. In this case, computation time of the S-UTD model is 2118.35 s, whereas the computation time of the S-UTD-CH model is 354.18 s. However, the difference between the relative path losses of models is only 0.06 dB. The S-UTD-CH model can be used instead of the S-UTD model with relatively less computation time. It is obvious that the S-UTD model needs the highest computation time.

In the second case, the operational frequency is 100 MHz and the distance between the obstacles is 50 m. The transmitter heights are selected as 10, 15, 20, 25 and 30 m, respectively. In order to show how the relative path loss is affected by the change of the distance between obstacles, simulation is performed, and the results are shown in Table 2.

In Table 2, the first column shows the transmitter height. Next three columns indicate the relative path loss of S-UTD-CH, S-UTD and UTD models, respectively. The latter three columns give the computation time of mentioned models. The eliminated obstacle number in the S-UTD-CH model is shown in the last column.

The UTD model requires the least computation

time. Due to that all the obstacles are in the Fresnel zone of the transmitter, there is no eliminated obstacle in the S-UTD-CH model. This situation leads the same computation times for the S-UTD-CH model and the S-UTD model.

In the third case, the transmitter height is 30 m and the distance between the obstacles is 25 m. The operational frequencies are selected as 100, 400, 900 and 1800 MHz, respectively. In order to indicate how the relative path loss is affected by the change of operational frequency, simulation is performed, and the results are illustrated in Table 3.

In Table 3, the first column shows the operational frequency. Next three columns indicate the relative path loss of S-UTD-CH, S-UTD and UTD models, respectively. The latter three columns give the computation time of mentioned models. The eliminated obstacle number in the S-UTD-CH model is shown in the last column.

The S-UTD model requires the most computation time with ultimate in accuracy. Also, in highly elevated (30 m) transmitting antenna cases, there is obstacle elimination. Moreover, as the operational frequency increases, eliminated obstacle number increases too. There is almost no difference between prediction accuracy of S-UTD and S-UTD-CH models. In these cases S-UTD-CH model can be used in multiple diffractions with regard to less computation time. Furthermore, as the operational frequency increases, predicted relative path loss decreases.

The second proof is made by using FEKO electromagnetic simulation software tool. The test scenario is given in Fig. 6.

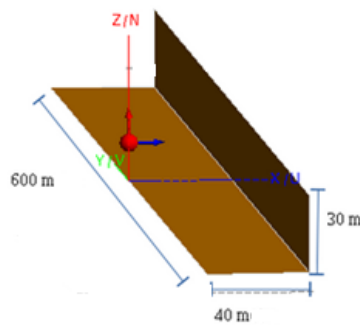


Fig. 6. The second test scenario.

Table 1: 1<sup>st</sup> Case (f = 100 MHz, d = 25 m)

Transmitter Height	S-UTD-CH RPL (dB)	S-UTD RPL (dB)	UTD RPL (dB)	S-UTD-CH Time (s)	S-UTD Time (s)	UTD Time (s)	Eliminated Obstacle
10	-52,91	-52,91	-86,82	1355,95	1319,92	4,16	0
15	-47,02	-47,02	-82,19	1303,26	1323,15	4,08	0
20	-38,98	-38,98	-75,9	2075,16	1953,81	5,62	0
25	-32,12	-32,12	-35,36	2044,41	1995,04	5,53	0
30	-27,99	-27,93	-29,49	354,18	2118,35	5,83	1

As can be seen in the Fig. 6, the transmitting antenna height is 15 m, and at a 40 m distance from the transmitter there is an obstacle whose height is 30 m. The operational frequency is 900 MHz. By using the FEKO coverage map is drawn in Fig. 7.

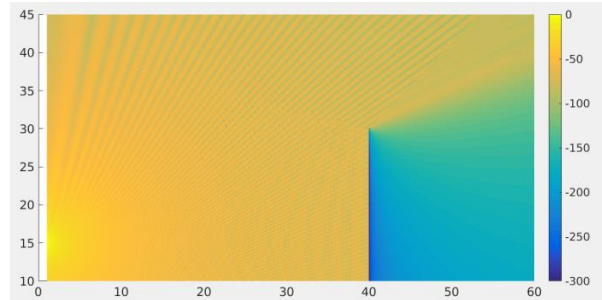


Fig. 7. FEKO simulation results.

As it is seen in the Fig. 7, in front of the obstacle there are LOS, ground reflected, obstacle reflected and backward diffracted waves. Thanks to that these rays are in different phases, interference pattern is observed in front of the obstacle. Moreover in behind of the obstacle, only diffracted waves are propagated.

Coverage map also generated with the S-UTD-CH model for the same scenario and this map is illustrated in Fig. 8.

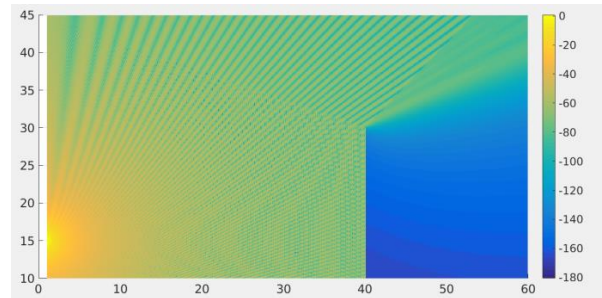


Fig. 8. S-UTD-CH simulation results.

As can be seen in the Fig. 8, the same interference pattern is obtained behind and in front of the obstacle. Behind the obstacle there is some difference resulted from FEKO design.

Table 2: 2<sup>nd</sup> Case (f = 100 MHz, d = 50 m)

Transmitter Height	S-UTD-CH RPL (dB)	S-UTD RPL (dB)	UTD RPL (dB)	S-UTD-CH Time (s)	S-UTD Time (s)	UTD Time (s)	Eliminated Obstacle
10	-46,56	-46,56	-81,7	1363,38	1361,64	4,29	0
15	-41,63	-41,63	-77,86	1303,6	1266,21	4,16	0
20	-30,8	-30,8	-35,33	2137,49	2119,73	5,73	0
25	-35,78	-35,78	-73,23	2122,38	2150,01	5,54	0
30	-26,80	-26,80	-29,35	2116,67	2150,26	5,88	0

Table 3: 3<sup>rd</sup> Case (Transmitter height = 30 m, d = 25 m)

Frequency (MHz)	S-UTD-CH RPL (dB)	S-UTD RPL (dB)	UTD RPL (dB)	S-UTD-CH Time (s)	S-UTD Time (s)	UTD Time (s)	Eliminated Obstacle
100	-27,99	-27,93	-29,49	354,18	2118,35	5,83	1
400	-30,43	-30,34	-30,45	55,12	2136,95	5,63	2
900	-31,78	-31,68	-31,57	2,04	2076,68	5,66	4
1800	-33,44	-33,67	-33,24	0,61	2101,19	5,54	5

#### IV. CONCLUSIONS

A top-down approach for S-UTD-CH model is presented in this study. A great many simulations indicates that there is tremendous contribution to UTD model in the case of multiple transition region diffraction. Adding the derivative of incoming field removes the discontinuity problem of UTD model in the transition zone. Actually, the UTD model can be used to predict the field strength or relative path loss in the rural or single diffraction case with a relatively short computing time. Next, the S-UTD model has ultimate accuracy with relatively long computing time in the multiple diffraction including more than 10 obstacles. Besides, there is a tradeoff between the accuracy of prediction and computation time. Afterwards, Slope UTD with a Convex-Hull (S-UTD-CH) model is based on the selection mechanism, based on the Fresnel zone concept and convex hull model, for unsuccessful obstacles. The S-UTD-CH model provides accurate results and short computation time in multiple-diffraction scenarios including more than 10. Moreover, due to the elevated transmitting antenna and higher operational frequency cases the relative path loss of models and contribution to the UTD model are reduced. Furthermore, verification of the S-UTD-CH model is provided by FEKO electromagnetic wave simulation software tool. To sum up, the S-UTD-CH model could be used in radio planning tool, broadcasting systems and prediction algorithms thanks to higher accuracy of prediction and less computation time.

#### ACKNOWLEDGMENT

This work is partially supported by TUBITAK (The Scientific and Technological Research Council of Turkey) under the Grant No. 215E360.

#### REFERENCES

- [1] V. A. Borovikov and B. E. Kinber, *Geometrical*

*Theory of Diffraction*. Institution of Electrical Engineers, London, UK, 1994.

- [2] J. B. Keller, "Geometrical theory of diffraction," *Journal of the Optical Society of America*, vol. 52, no. 2, pp. 116-130, 1962.
- [3] C. A. Balanis, L. Sevgi, and P. Y. Ufimtsev, "Fifty years of high frequency diffraction," *International Journal of RF and Microwave Computer-Aided Engineering*, vol. 23, no. 4, pp. 1-6, 2013.
- [4] M. Schneider and R. J. Luebbers, "A uniform double diffraction coefficient," *Antennas and Propagation Society International Symposium*, San Jose, CA, vol. 3, pp. 1270-1273, June 1989.
- [5] R. J. Luebbers, "Finite conductivity uniform GTD versus knife edge diffraction in prediction of propagation path loss," *IEEE Transactions on Antennas Propagation*, vol. 32, no. 1, pp. 70-76, 1984.
- [6] L. J. Graeme, *Geometrical Theory of Diffraction for Electromagnetic Waves*. Institution of Electrical Engineers, London, UK, 1976.
- [7] J. Deygout, "Multiple knife-edge diffraction of microwaves," *IEEE Transactions on Antennas Propagation*, vol. 14, no. 4, pp. 480-489, 1966.
- [8] J. Walfisch and H. L. Bertoni, "A theoretical model of UHF propagation in urban environment," *IEEE Transactions on Antennas Propagation*, vol. 36, no. 12, pp. 1788-1796, 1988.
- [9] C. Tzaras and S. R. Saunders, "Comparison of multiple-diffraction models for digital broadcasting coverage prediction," *IEEE Transactions on Broadcasting*, vol. 46, no. 3, pp. 221-226, 2000.
- [10] R. G. Kouyoumjian and P. H. Pathak, "Uniform geometrical theory of diffraction for an edge in a perfectly conducting surface," *Proceedings of IEEE*, vol. 62, no. 11, pp. 1448-1461, 1974.
- [11] E. Yazgan, "A simple formulation of UTD for some reflector antennas," *International Journal of*

- Electronics*, vol. 66, no. 2, pp. 283-288, 1989.
- [12] A. Kara and E. Yazgan, "Roof shape modelling for multiple diffraction loss in cellular mobile communication systems," *International Journal of Electronics*, vol. 89, no. 10, pp. 753-758, 2002.
- [13] J. B. Andersen, "Transition zone diffraction by multiple edges," *IEEE Proceedings Microwave Antennas and Propagation*, vol. 141, no. 5, pp. 382-384, 1994.
- [14] J. B. Andersen, "UTD multiple-edge transition zone diffraction," *IEEE Transactions on Antennas and Propagation*, vol. 45, no. 7, pp. 1093-1097, 1997.
- [15] K. Rizk, R. Valenzuela, D. Chizhik, and F. Gardiol, "Application of the slope diffraction method for urban microwave propagation prediction," *IEEE Vehicular Technology Conference*, Ottawa, Ont., vol. 2, pp. 1150-1155, May 1998.
- [16] C. Tzaras and S. R. Saunders, "An improved heuristic UTD solution for multiple-edge transition zone diffraction," *IEEE Transactions on Antennas Propagation*, vol. 49, no. 12, pp. 1678-1682, 2001.
- [17] L. Vogler, "An attenuation function for multiple knife-edge diffraction," *Radio Science*, vol. 17, no. 6, pp. 1541-1546, 1982.
- [18] A. Kara, E. Yazgan, and H. L. Bertoni, "Limit and application range of slope diffraction for wireless communication," *IEEE Transactions on Antennas Propagation*, vol. 51, no. 9, pp. 2514-2514, 2003.
- [19] M. B. Tabakcioglu and A. Kara, "Comparison of improved slope UTD method with UTD based methods and physical optic solution for multiple building diffractions," *Electromagnetics*, vol. 29 no. 4, pp. 303-320, 2009.
- [20] M. B. Tabakcioglu and A. Kara, "Improvements on slope diffraction for multiple wedges," *Electromagnetics*, vol. 30, no. 3, pp. 285-296, 2010.
- [21] M. B. Tabakcioglu, D. Ayberkin, and A. Cansiz, "Comparison and analyzing of propagation models with respect to material, environmental and wave properties," *ACES Journal*, vol. 29, no. 6, pp. 486-491, 2014.
- [22] M. B. Tabakcioglu and A. Cansiz, "Application of S-UTD-CH model into multiple diffraction scenarios," *International Journal of Antennas and Propagation*, vol. 2013, pp. 1-5, 2013.
- [23] M. B. Tabakcioglu, "S-UTD-CH model in multiple diffractions," *International Journal of Electronics*, vol. 103, no. 5, pp. 765-774, 2015.
- [24] R. J. Luebbers, "A heuristic UTD slope diffraction coefficient for rough lossy wedges," *IEEE Transactions on Antennas and Propagation*, vol. 37, no. 3, pp. 206-211, 1989.
- [25] D. A. McNamara, C. V. Pistorious, and J. A. G. Malherbe, *Introduction to the Uniform Geometrical Theory of Diffraction*. Boston, MA: Artech House, 1990.
- [26] K. Karousos and C. Tzaras, "Multi time-domain diffraction for UWB signals," *IEEE Trans. Antenna Propagation*, vol. 56, no. 5, pp. 1420-1427, 2008.
- [27] G. Koutitas and C. Tzaras, "A slope UTD solution for a cascade of multishaped canonical objects," *IEEE Trans. Antenna Propagation*, vol. 54, no. 10, pp. 2969-2976, 2008.
- [28] A. Tajvidy and A. Ghorbani, "A new uniform theory-of-diffraction-based model for the multiple building diffraction of spherical waves in microcell environments," *Electromagnetics*, vol. 28, no. 5, pp. 375-387, 2008.
- [29] O. M. Bucci, "The experimental validation of a technique to find the convex hull of scattering systems from field data," *IEEE Antennas and Propagation Symposium*, pp. 539-542, 2003.
- [30] H. K. Chung and H. L. Bertoni, "Application of isolated diffraction edge method for urban microwave path loss prediction," *IEEE Vehicular Tech. Conf.*, pp. 0205-209, 2003.
- [31] H. L. Bertoni, *Radio Propagation for Modern Wireless Systems*. Prentice Hall, 2000.
- [32] G. Liang and H. L. Bertoni, "A new approach to 3-D ray tracing for propagation prediction in cities," *IEEE Transactions on Antennas and Propagation*, vol. 46, no. 6, pp. 853-863, 1998.
- [33] O. Ozgun and L. Sevgi, "Comparative study of analytical and numerical techniques in modeling electromagnetic scattering from single and double knife-edge in 2D ground wave propagation problems," *ACES Journal*, vol. 27, no. 5, pp. 376-388, 2012.
- [34] A. Skarlatos, R. Schuhmann, and T. Weiland, "Simulation of scattering problems in time domain using a hybrid FDTD UTD formulation," *The 19th Annual Review of Progress in Applied Computational Electromagnetics*, 2003.
- [35] P. Persson, "Modeling conformal array antennas of various shapes using uniform theory of diffraction (UTD)," *ACES Journal*, vol. 21, no. 3, pp. 305-317, 2006.
- [36] G. Apaydin and L. Sevgi, "A novel wedge diffraction modeling using method of moments (MoM)," *ACES Journal*, vol. 30, no. 10, pp. 1053-1058, 2015.
- [37] M. A. Uslu, G. Apaydin, and L. Sevgi, "Double tip diffraction modeling: Finite difference time domain vs. method of moments," *IEEE Trans. on Antennas and Propagat.*, vol. 62, no. 12, pp. 6337-6343, 2014.
- [38] O. Ozgun and L. Sevgi, "Double-tip diffraction modeling: Finite element modeling (FEM) vs. uniform theory of diffraction (UTD)," *IEEE Trans. on Antennas and Propagat.*, vol. 63, no. 6, pp. 2686-2693, 2015.



**Mehmet Baris Tabakcioglu** was born in 1981. He received B.S. degree in Physics from Middle East Technical University in 2005. Then he received the M.S. degree in Electrical and Electronics Engineering from Atılım University in 2009. After that he received the Ph.D degree in Electrical and Electronics Engineering from Atatürk University in 2013.

His currently research area is wave diffraction, reflection and propagation. He is currently working at Bursa Technical University in Electrical and Electronics Engineering department.